http://dx.doi.org/10.11142/jicems.2013.2.1.45
Journal of International Conference on Electrical Machines and Systems Vol. 2, No.1 , pp.45 ~50 , 2013

Effects of Resistivity Variation in a Very Low Temperature on the Characteristics of Induction Motors

Beom Jin Kim*, Jin Sung Kimand Gwan Soo Park***

Abstract –This paper presents design of induction motor in very low temperature for LNG main cargo pump and comparison of two motors. One is the motor for using in room temperature and another is the motor for using very low temperature. This paper designs with Equivalent circuit Method and uses Finite Element Method to analysis. The motor for very low temperature considers variation of coil resistivity due to temperature change and compare torque characteristic with the motor for room temperature. Design element of motor for very low temperature considers resistivity variation following temperature change on going through this paper. The result shows that two types of motors are almost same torque curve characteristic even though they are not the same environment.

Keywords: LNG, Main cargo pump, Characteristic curve, Induction motor

1. Introduction

Alternative fuel has been interested in prevention of environmental pollution, increasing demand for cleaner fuel, and diversification policy of energy resources. Among them, LNG is more economical than fossil fuel and abundant reserves. Hence, a LNG Cargo ship that carries LNG is increasing to meet a rate of LNG demand [1-3].

In the ship, there is a motor in LNG Main Cargo Pump to transfer Liquefied natural gas as -163℃. To operate in very low temperature, induction motor is used in Cargo Pump instead of Permanent Magnet motor. Therefore, induction motor was designed in this this paper considering a variation of resistivity of rotor bar in very low temperature.

To derive an analysis of motor characteristics, equivalent circuit method and FEM are used for deriving motor torque characteristic curves. The study presents the analysis of electro-magnetic material characteristic at very low temperature and shows having similar torque characteristics between motors for room temperature. As well, there is a motor for reduction of cross-section area for the motor as well as a decrease of resistivity at very low temperature [4-5].

2. Material Characteristic change in -163℃

The core of the induction motor for LNG Main cargo pump uses the silicon steel 50PN400. The silicon steel is the ferromagnetic characteristic. When inducing the magnetic field to the silicon steel, the magnetic moments of material atom array to the magnetic field direction. However, the thermal vibration generated following external temperature interrupts the magnetic moments array following the magnetic field. Hence, the magnetic field direction arrays partially following temperature and then appears litter permeability more increasing temperature.

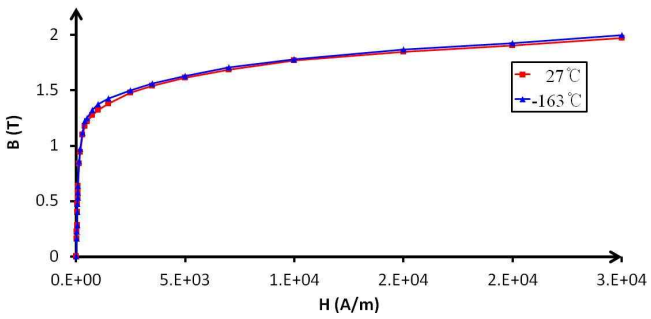

Fig. 1. The magnetic curve change following temperature

Change of magnetic curve following the silicon steel temperature is shown as Fig. 1. Due to the thermal vibration interrupting the magnetic moments in -163℃ is smaller than in room temperature, the magnetic characteristic relatively have great characteristic, however, the value of change is not big different in room temperature. On the basis of this paper, the core does not take into account the magnetic characteristic with which an induction motor is designed.

* School of Electrical Engineering, Pusan National University, Korea. (beomjin@pusan.ac.kr, gspark@pusan.ac.kr)
** LSIS Co., Ltd, Korea (jskimm@lsis.biz)
Received 08 February 2013; Accepted 20 February 2013

To get the metal temperature following the resistivity, the first thing is the resistivity following temperature using the resistivity in room temperature and the resistivity coefficient per unit temperature could use Eq. (1) [6].

$$\rho = \rho_0[1+\alpha_0(t-t_0)] \quad (1)$$

where ρ is the resistivity at temperature T℃, ρ_0 is the resistivity at 0℃, α_0 is the resistivity coefficient per unit temperature, t is random temperature and t_0 is 0℃.

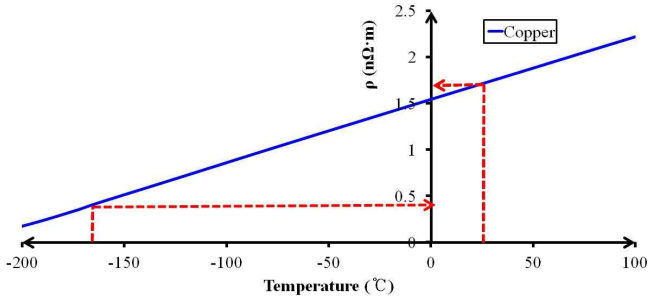

Fig. 2. The resistivity change of the copper following temperature

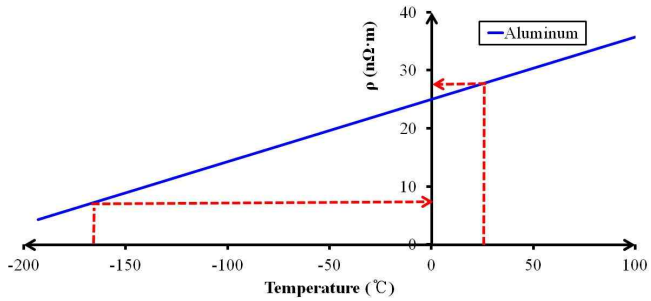

Fig. 3. The resistivity change of the aluminum following temperature

Fig.2 and Fig.3 show the resistivity of the copper for using the stator coil and the aluminum for using the rotor bar following temperature, respectively. The resistivity of the copper decreases 1.725 nΩ·m to 0.423 nΩ·m and the aluminum decreases 27.9 nΩ·m to 7.511 nΩ·m.

For the motor, the material characteristic changes in very low temperature. The permeability of the silicon steel increases and the copper and the aluminum resistivity following temperature change are confirmed to decrease. However, the rate of the resistivity change is more than the rate of the permeability change. Hence, in this paper, the induction motor is designed by considering resistivity change.

3. Torque characteristic analysis following temperature change

This paper is designed 640kW 3-phase induction motor for using in room temperature. The induction motor is LNG Main cargo pump in LNG cargo ship and the squirrel cage type using aluminum bars. The input voltage is 6600 V and the motor rotates 1800 rpm with 4-poles. Table 1 is shown the induction motor's design specification. The motor efficiency is 91 %. This efficient is the standard of IACS (International Association of Classification Societies). Therefore, this study designs to aim 91 % efficiency.

The resistivity change of the stator winding and the rotator bar presents the change of primary and secondary resistance in the equivalent circuit for the induction motor. Due to the change of the copper and the aluminum has big different in 163℃, primary and secondary resistances are considered to be proportional to them. Table 2 shows that the equivalent circuit constants compare with changing temperature for calculating the motor characteristic. The primary and the secondary resistance respectively confirm in room temperature and very low temperature and the resistance in -163℃ decreases a quarter than in 27℃.

Table 1. The design specification for the induction motor

Requirement	Value
Type	Vertical Submerged 3-Phase Induction
Rated Output	640 kW
Synchronous Speed	1800 rpm
Electric Power Source	AC 6600 V
Efficiency	91 %
Frequency	60 Hz
Cooling Liquid	LNG

Table 2. The Comparison of the equivalent circuit following temperature

Equivalent circuit parameter	27℃	-163℃
R_1	0.176 Ω	0.048 Ω
R_2	1.580 Ω	0.412 Ω
X_1	6.424 Ω	6.42 Ω
X_2	6.741 Ω	7.38 Ω
g_0	7323.56 ℧	7321.29 ℧
b_0	62.85 ℧	62.13 ℧

From the equivalent circuit parameter, the torque is confirmed by Eq. (2) [7]. The primary winding resistance and the secondary aluminum bar resistance variations are given by the variation of generating the torque following rotating speed.

$$T = \frac{m}{\omega_s} \times V_1^2 \times \frac{(R_2/s)}{[R_1 + (R_2/s)^2] + (X_{l1} + X_{l2})^2} \quad (2)$$

where m is the phase, ω_s is the velocity angular, V_1 is the input voltage, R_1 is the primary resistance, R_2 is the secondary resistance, X_{l1} is the primary leakage reactance, X_{l2} is the secondary leakage reactance and s is the slip.

By using the equivalent circuit parameters, the torque cha racteristic of 640 kW motor following temperature presents Fig. 4. The stating torque at very low temperature reduces more than at room temperature. However, the magnitude of the rate torque is better than the torque at room temperature [8].

On the base of the equivalent circuit parameters and the torque characteristic, the output power, the efficiency, the torque and so on of the induction motor present in Table 3. In room temperature, the slip is smaller than in very low temperature and loss decreases and efficiency increases.

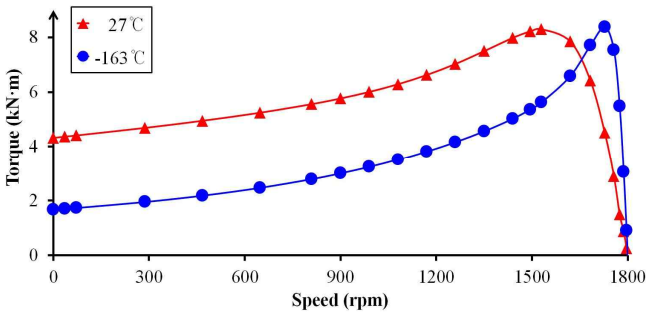

Fig. 4. Comparing torque-speed curve at 26℃ and -163℃

4. FEM Analysis following temperature change

The design of characteristic analyzes to use 2D FEM. The Characteristic at room temperature and very low temperature compares using the values of resistivity of calculating line resistance per phase at room temperature and at very low temperature [9].

The flux line following temperature is shown as Fig. 5 and 6 and the flux density distribution is shown as Fig. 7 and 8. From Fig. 7 and 8, Table 4 presents the value of each place about flux density. Due to decreases the resistivity in very low temperature comparing with in room temperature, the current inducing the same input voltage is much higher than in room temperature. Therefore, the flux density is relatively much high in very low temperature.

5. Design of motor for using in -163℃ considering the change of resistivity

The resistivity of copper for stator slot and aluminum for rotor slot are changed by temperature shown as Fig. 9. Although the motor has the same shape, there is different characteristic generating in very low temperature following change of resistivity. Eq. (3) shows that the resistance at 27℃ and following cross-section change are similar [10].

Table 3. Operating characteristic at 27℃ and -163℃

Operating Characteristic	27℃	-163℃
Output Power	640 kW	640 kW
Rated Slip	0.03	0.008
Resistance of ST	0.176 Ω	0.0484 Ω
Core Loss	4660.07 W	4677.07 W
I^2R Loss Stator	4366.11 W	1180.04 W
I^2R Loss Rotor	19573 W	5115.67 W
Mech. Loss	40.7537 W	41.67 W
Stray Loss	9600 W	9600 W
Total Loss	38239.9 W	20614.4 W
Efficiency	94.36 %	96.879 %
Power Factor	64.4 %	63.15 A
Current of ST	53.37 A	54.37 A
No-Load Current	18.24 A	18.528 A
Rated Torque	3499.04 N·m	3421.9 N·m
Starting Torque	4311.21 N·m	1671.71 N·m
Rated Speed	1746.6 rpm	1785.72 rpm

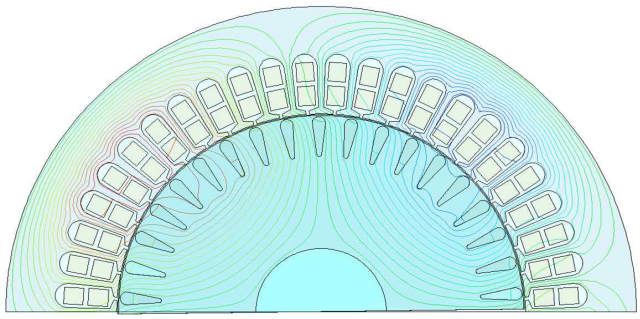

Fig. 5. Magnetic flux line of the motor at 27℃

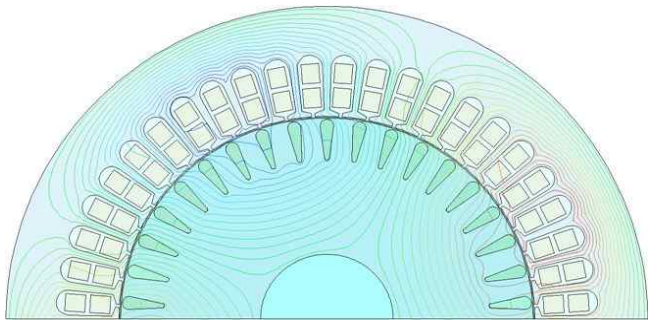

Fig. 6. Magnetic flux line of the motor at -163℃

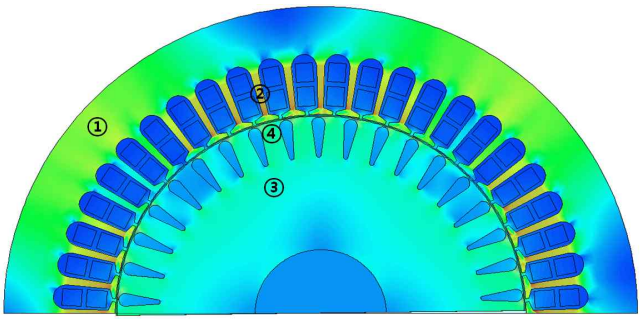

Fig. 7. Flux density distribution of motor at 27℃

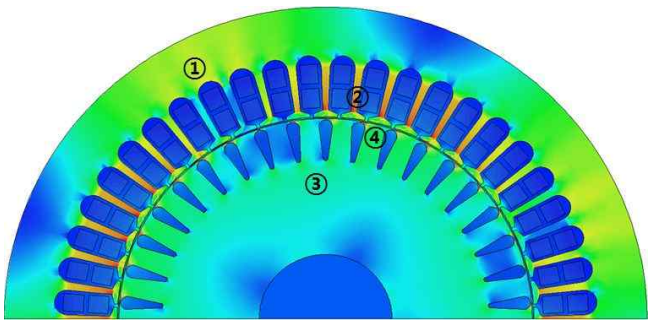

Fig. 8. Flux density distribution of motor at -163℃

$$R = \rho_{27℃} \times \frac{N_{ph} \times l}{A}$$
$$R' = \rho_{163℃} \times \frac{N_{ph} \times l}{A'} \quad (3)$$
$$R \approx R'$$

Table 4. The each area of flux density at 27℃ and -163℃

Flux density on analysis area		B (27℃)	B (-163℃)
Stator back yoke	①	1.64 T	1.54 T
Stator teeth	②	2.07 T	2.11 T
Rotor back yoke	③	0.88 T	0.75 T
Rotor teeth	④	0.96 T	1.27 T
Air gap		0.55 T	0.53 T

where R is the resistance at 27℃, R' is the resistance following cross-section change and N_{ph} is the winding number per phase. By using Eq. (3), cross-area regarding the stator and the rotor slot reduces considering the resistivity change in very low temperature.

Fig. 9 shows that slot area decrease in following the motor design for using very low temperature. The solid line and dotted line present the induction motor for using room temperature and very low temperature, respectively. The stator slot area in room temperature is 846 mm^2 and the stator slot area considering the resistivity reduction is 290.41 mm^2. It reduces about 67 %. Also, the rotor slot area in room temperature is 243 mm^2 and the rotor slot area considering the resistivity change rate is 65.18 mm^2. It reduces about 73 %.

As mentioned earlier, due to reduce the slot area following the design for using in very low temperature, the whole shape is quite different. Fig. 10 shows the general shape both of them. The inner and outer change of induction motor for using two type of temperature arrange in Table 5.

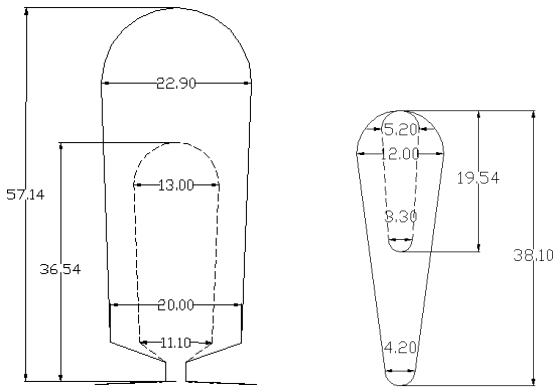

(a) Stator (b) rotor

Fig. 9. Comparing the stator and rotor slot area

Table 5. Comparing the volume of induction motor

Designed value	27℃	-163℃
Stator outer diameter	580 mm	455.34 mm
Stator inner diameter	376 mm	287.14 mm
Rotor outer diameter	372.7 mm	283.84 mm
Rotor inner diameter	120 mm	120 mm
Air gap distance	1.65 mm	1.65 mm
Volume change rate	100 %	61.5 %

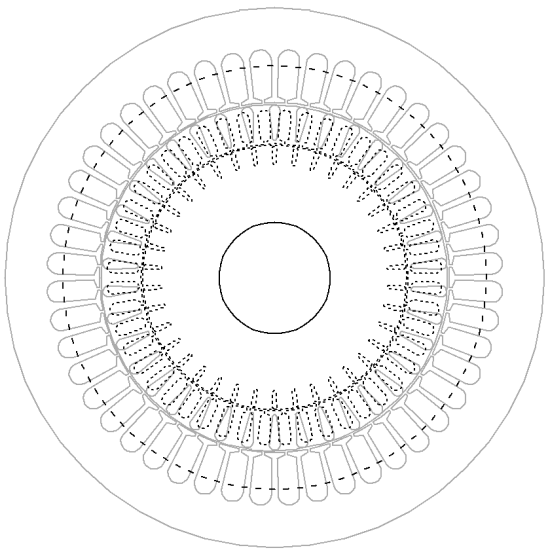

Fig. 10. Comparing the stator and rotor in the whole shape

6. FEM Analysis for the designed motor for using in -163℃

The flux density distribution calculates on 1.3 sec using FEM analysis software after starting the motor speed 1746.59 rpm as same as the motor driving in room temperature. The flux line and flux density distribution of designed motor for using in very low temperature is shown as Fig. 11. Also, the value of each area about flux density arranges in Table 6 comparing two types of temperature.

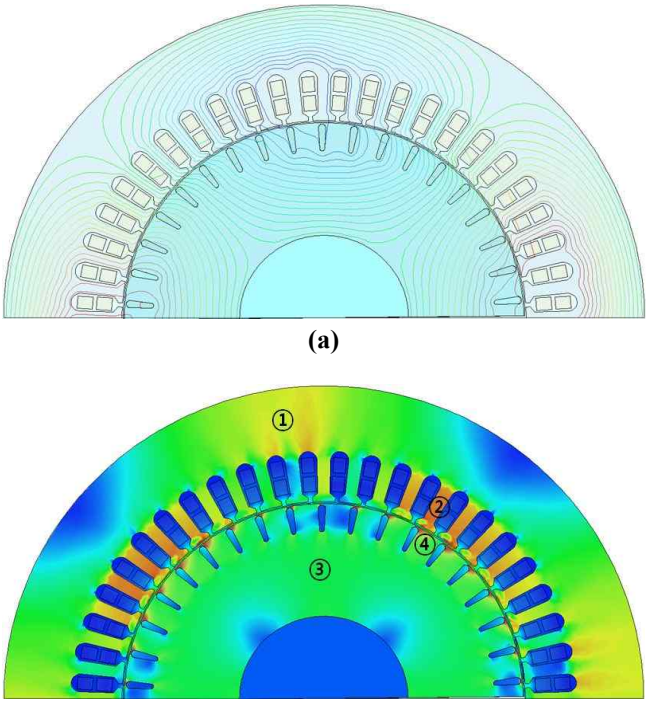

(a)

(b)

Fig. 11. Designed the motor for using in -163℃ by FEM (a) The flux line, (b) the flux density distribution

Table 6. Comparing flux density of the each motors

Flux density on analysis area		B(27℃)	B (-163℃)
stator back yoke	①	1.64 T	1.58 T
Stator teeth	②	2.07 T	1.86 T
Rotor back yoke	③	0.88 T	1.02 T
Rotor teeth	④	0.96 T	1.1 T
Air gap		0.55 T	0.69 T

Table 6 shows that the flux density of the rotor teeth in very low temperature confirms to be similar to the flux density in room temperature. It is clear that the result of design applied electrical characteristic following temperature change is satisfactory fine. Due to fix the outer diameter of rotor, the cross-section of stator could not reduce to be proportional to decrease resistivity of winding. Hence, On the some part of the flux density at -163℃ is smaller than at 27℃ because of increment of the whole resistance.

The torque characteristic of the induction motor for using in very low temperature is similar to the other for using in room temperature due to reduce the area considering the resistance of the motor for using at 27℃. To get the average torque, FEM analysis is used. Fig. 12 shows that two torque are similar ever if they are not a same temperature. The stating torque is about 5.53 kN·m and the rate torque is about 3.434 kN·m. The stating torque increases to compare with the torque for room temperature and the rate torque is decreased. The reason is the same as the flux density is small on some part.

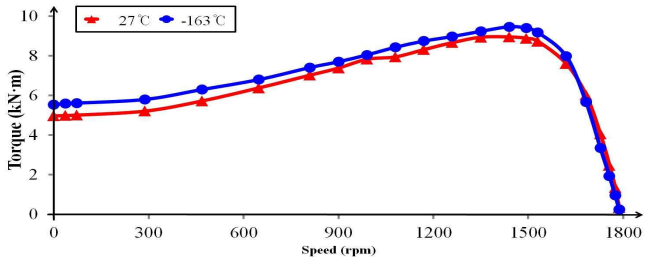

Fig. 12. Comparing the torque-speed curve of low temperature design motor and room temperature design motor

7. Conclusion

In this paper, the study presents the design of using LNG main cargo pump induction motor in very low temperature. Consequently, the designed motor could reduce the price to manufacturing and it is much smaller than it for using room temperature. Therefore, the result shows that the size could be reduced for effective pumping in the optimum design without any performance loss compare to the room temperature.

Acknowledgements

This research was supported by Basic Science Research Program through the National Research Foundation of Korea(NRF) funded by the Ministry of Education, Science and Technology(2010-0006864)

References

[1] Ruch. S, "Submerged Motor LNG Pumps in Send-out System Service," Pumps&System, pp. 32-37, May 2004.

[2] Toshitaro Takeuchi, "Electrical Machine Design," Ohmsha Ltd, , pp. 117-144, 1979.
[3] B.D. Cullity, "Introduction to Magnetic Materials," ITC, pp. 113-152, 1991.
[4] P. Shcherbakov, I. Bogdanov, S. Kozub, L TKachenkoStephen, "Magnetic Properties of Silicon Electrical Steels and Its Application in Fast Cycling Superconducting magnets at low temperatures," RuPAC, pp. 298-300, 2004.
[5] Tim Rahill, Jeff Hudson, "Application of Temperature ratings for Industrial Electric Induction Motors," *IEEE* Paper No. PCIC-2006-5, pp. 1-11, 2006.
[6] S.O. Kasap, "Principles of Electronic Materials and Devices," Mcgraw Hill, pp.111-118, 2002.
[7] P. C. Sen, "Principles of Electric Machines and Power Electronics.", John Wiley.
[8] Mohamed El Hachemi Benbouzid, "A review of Induction Motors Signature Analysis as a Medium for Faults Detection", *IEEE TRANS. Industrial Electronic*, pp.984-993, 2000.
[9] C.C. Chan, Lieong Yan, Pozhang Vhen, Zezgong Wang, K.T. Chau, "Analysis of electromagnetic and thermal fields for Induction Motors during starting", IEEE Trans. On Energy Conversion, Vol.9, No.1, pp.53-60, 1994.
[10] J. Kolowrotkiewicz, M. Baranski, W. Szeleg, and, L. Dlugiewicz, "FE Analysis of Induction Motor Working in Cryogenic Temperature," The International Journal for Computation and Mathematics in Electrical and Electronic Engineering, Vol. 26 No 4, pp.952-964, 2007.

Beom Jin Kim received B.S degree in Electrical Engineering from Dong-A University, Busan, Korea. He entered the Collage of Electro-electrical engineering in Pusan National University, Busan, Korea, to study toward the Master degree. His research interests are designing Electric Machines and analyzing Finite Element Method.

Jin Sung Kim received B.S degree in Nano Engineering from In-je University and his M.S. degree from Pusan National University of Electro-electrical engineering, Busan, Korea. He is currently an engineer for Ultra high voltage transformer design working in LSIS Co., Ltd.

Gwan Soo Park received his B.S. degree from Seoul National University, Seoul, Korea in 1985, and his M.S. degree from Seoul National University of Electrical Engineering, Seoul, Korea in 1987, and his Ph.D. degree in Electrical Engineering from Seoul National University, Seoul, Korea in 1992. He is now working with Pusan National University and his research interests are Application of Electric Machines and Electromagnetic Devices.